

Giant negative photoconductivity in $\text{La}_{0.7}\text{Ca}_{0.3}\text{MnO}_3$ thin films

V. Moshnyaga, A. Giske, and K. Samwer

I. Physikalisches Institut, Universität Göttingen, Tammannstrasse 1, D-37077 Göttingen, Germany

E. Mishina, T. Tamura, and S. Nakabayashi

Department of Chemistry, Faculty of Science, Saitama University, 255 Shimo-okhubo, Saitama 338-8570, Japan

A. Belenchuk, O. Shapoval, and L. Kulyuk

Institute of Applied Physics, Academy of Sciences, Street Academiei 5, MD-2028 Chisinau, Moldova

(Presented on 9 January 2004)

The increase of the resistance up to two orders of magnitude under laser illumination ($\lambda = 760$ nm) was observed in $\text{La}_{0.7}\text{Ca}_{0.3}\text{MnO}_3$ (LCMO) epitaxial thin films in ferromagnetic state. Optical absorption also increases by 10–15 % and the magnetic second-harmonic generation signal decreases down to zero under the irradiation. The light induced changes are reversible with characteristic relaxation times $\tau \sim 1-30$ s. Magnetic field, $B = 4$ T, suppresses the photoconductivity and decreases its relaxation time. Photoinduced effects are caused by the injection of a large number of extra carriers, which change the (antiferromagnetic) AFM/FM phase balance in LCMO, favoring the insulating AFM state. © 2004 American Institute of Physics. [DOI: 10.1063/1.1687555]

Complex phase diagram in perovskite manganites¹⁻³ is governed by two main interactions: double exchange,⁴ which favors ferromagnetic (FM) metallic state, and electron lattice interaction (Jahn–Teller effect),⁵ which results in antiferromagnetic (AFM) charge ordered insulator (COI). It was argued⁶ that the competition between the AFM and FM phases in the presence of disorder results in electronic phase separation (EPS) and percolative electron transport. EPS develops on the nanometer (submicrometer) scale as was observed by scanning tunneling microscopy.^{7,8} Colossal magnetoresistance (CMR) was thus viewed⁹ as magnetic field induced percolation in an electronically inhomogeneous medium; the current path is switched by the field, which favors FM metallic phase and suppresses AFM insulating one.¹⁰

An attractive way to study phase transformations seems to be optical injection of extra carriers. A decrease of the resistance under laser irradiation with very short relaxation times $\tau \sim 150$ ps for $T > T_C$ in a $\text{La}_{0.7}\text{Ca}_{0.3}\text{MnO}_3$ (LCMO) film⁹ was interpreted as a photoionization of the Jahn-Teller (JT) small polarons. For $T < T_C$ the resistance increases under irradiation and the relaxation becomes slower, $\tau = 1-10$ ns, indicating the excitation of magnons. Photoinduced change of optical absorption also changes with $\tau \sim 100$ ns under the pulsed laser irradiation,¹⁰ that was interpreted as formation of Col clusters. For $(\text{Nd}_{0.5}\text{Sm}_{0.5})_{0.6}\text{Sr}_{0.4}\text{MnO}_3$ (Ref. 11) a photoinduced demagnetization manifests within 200 ps after laser pulse and the spin correlation recovers in 300 ns. Moreover, the COI/AFM ground state in “dark” for $\text{Pr}_{0.7}\text{Ca}_{0.3}\text{MnO}_3$ transforms into a FM metallic state after 10–100 μs of the laser irradiation.^{12,13}

We studied the transients of the photoconductivity (PC), optical absorption, and second-harmonic generation (SHG) in epitaxial $\text{La}_{0.7}\text{Ca}_{0.3}\text{MnO}_3/\text{MgO}(100)$ films on the time

scale 1–100 s for temperatures 90–300 K and magnetic field $B = 0, 4$ T. The films were prepared by a metal-organic aerosol deposition (MAD) technique.¹⁴ Single LCMO film with a thickness $d = 120$ nm (sample A) and a trilayer structure $\text{LCMO}(15 \text{ nm})/\text{MgO}(5 \text{ nm})/\text{LCMO}(15 \text{ nm})/\text{MgO}(100)$ (B) were studied. Perfect crystalline structure was confirmed by x-ray diffraction.¹⁵ The films show $T_C = 260$ K (A) and 250 K (B), accompanied by very sharp magnetic, $(1/M) \times (dM/dT) = 25\%/K$, and resistive, $(1/R)(dR/dT) = 15\%/K$, transitions measured by a superconducting quantum interference device magnetometer and four-probe dc measurements, respectively. For optical and photoelectric measurements the beam of an $\text{Al}_2\text{O}_3:\text{Ti}$ laser ($\lambda_\omega = 760$ nm, $\Delta t_{\text{pulse}} = 100$ fs, repetition rate 82 MHz, average power up to 1 W) was focused onto a spot of about 50 μm . The sample was placed in an optical nitrogen-flow cryostat inside the superconducting magnet. Transmission geometry was used with the angle of incidence of 45°; magnetic field was parallel to the light propagation direction. Two signals were measured simultaneously: transmission at λ_ω and SHG signal at $\lambda_{2\omega}$. The details of the SHG experiments are reported elsewhere.¹⁶

The resistivity ρ of the samples in dark and under laser irradiation for $B = 0$ and $B = 4$ T as a function of temperature are shown in Fig. 1. Dark $\rho(T)$ shows classical CMR: metal-insulator transition occurs at $T_{\text{MI}} = 250$ K (A) and 230 K (B), and magnetic field ($B = 4$ T) decreases ρ , yielding CMR = 100% $\times [(\rho(0) - \rho(B))/\rho(0)] \approx 90\%$ with a sharp maximum in the vicinity of T_{MI} . The laser illumination leads to a drastic increase of ρ for $T < T_C$ yielding maximal photoconductivity, $\Delta R/R_{\text{dark}} = 100\% \times (\rho_{\text{dark}} - \rho_{\text{light}})/\rho_{\text{dark}}$, of -600% (A) and $-10^4\%$ (B). CMR decreases under irradiation and its temperature distribution shifts to lower temperatures. The thinner film B shows no metallic behavior under

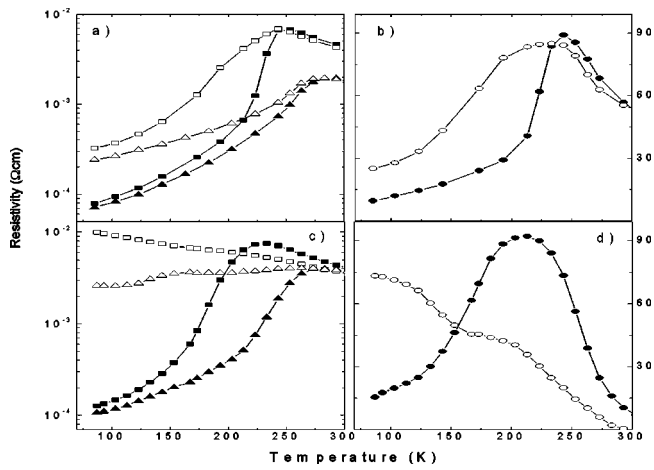


FIG. 1. Electrical resistivity ρ and $\text{CMR} = 100\% \times [\rho(0) - \rho(4T)] / \rho(0)$ as a function of temperature for a LCMO film with thickness 120 nm [Figs. 1(a) and 1(b), respectively] and for a trilayer structure LCMO(15 nm)/MgO(7 nm)/LCMO(15 nm) [Figs. 1(c) and 1(d)]. Closed and open symbols denote ρ values in dark and under illumination, respectively. Square symbols refer to the ρ values at zero (ambient) magnetic field, $B=0$, and triangles denote $\rho(B=4\text{ T})$. Closed and open circles relate to the CMR data in dark and under irradiation, respectively.

irradiation at zero field and behaves rather insulating with $d\rho/dT < 0$ for $T=90\text{--}300\text{ K}$. Note, the heating of the film by laser irradiation plays a minor role due to very short ($\Delta t = 100\text{ fs}$) pulses and repetition rate ($\Delta t = 13\text{ ns}$), which prevent the excitation of phonons. Moreover, maximal change of resistance is observed at the lowest $T=90\text{ K}$ where the heating effect is negligible due to the smallest value of dR/dT . Resistivity transients for film A are shown in Fig. 2. The relaxation of the photoconductivity is described by exponential form, $\Delta R(t) \sim \exp(-t/\tau)$, with decay times, $\tau \sim 1\text{--}30\text{ s}$, depending on the temperature and magnetic field. For $T > T_C$ and $B=0$ the relaxation is relatively fast, $\tau = 1.6\text{ s}$, while τ increases up to $\tau = 22\text{ s}$ at $T=90\text{ K}$. Magnetic field, $B=4\text{ T}$, enhances the relaxation of the photoconductivity, yielding a decrease of τ down to 6 s at T

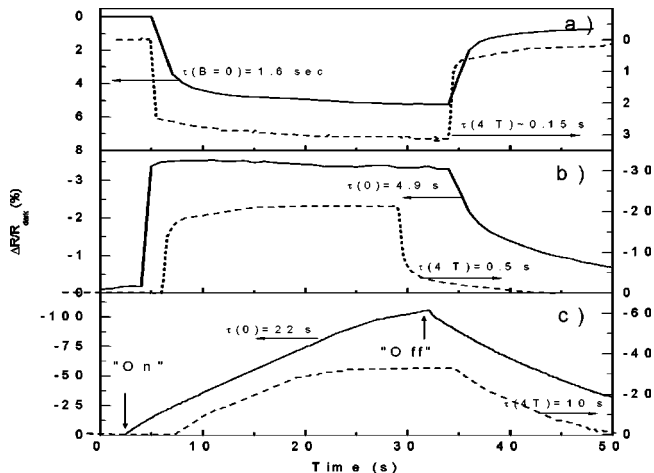


FIG. 2. Photoconductivity, $\Delta R/R_{\text{dark}} = (R_{\text{dark}} - R_{\text{light}}) / R_{\text{dark}}$, transients for a LCMO film obtained at $B=0$ and $B=4\text{ T}$ for paramagnetic region at $T=300\text{ K}$ (a), in the vicinity of the metal-insulator transition $T=250\text{ K}$ (b), and for ferromagnetic phase $T=90\text{ K}$ (c).

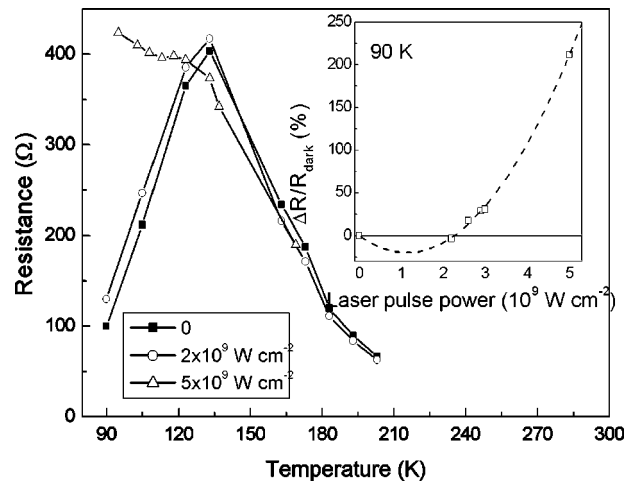


FIG. 3. The temperature dependence of the resistance in a LCMO film with $T_{\text{MI}} \approx 140\text{ K}$ for different values of laser pulse power. The inset shows the photoconductivity, $\Delta R/R_{\text{dark}}$, as a function of laser pulse power for $T=90\text{ K}$.

$=90\text{ K}$. Even for $T=300\text{ K}$ magnetic field still affects τ —it falls down at least to about 0.15 s, which was the limit of our measurement setup. Note that ρ decreases under illumination in the paramagnetic region, resulting in a positive photoconductivity, and increases for $T < T_C$ (negative photoconductivity). Nonlinear behavior of the photoconductivity on the laser pulse power J can be clearly seen in Fig. 3, where $R(T)$ curves for a LCMO film with low $T_{\text{MI}}=140\text{ K}$ are shown. For relatively low J minor changes of the resistance were observed in the ferromagnetic region. Only for $J > 2.5 \times 10^9\text{ W/cm}^2$ the photoconductivity shows a clear increase as seen in the inset of Fig. 3, where the dependence of the photoconductivity on the power for $T=90\text{ K}$ is depicted. Experimental points can be fitted by a quadratic function, $\Delta R \sim J^2$. Moreover, the sign of the photoconductivity depends on the laser power. For $J \approx 2.2 \times 10^9\text{ W/cm}^2$ we detected reliably $\sim 1\%$ decrease of the resistance rather than increase observed for higher fluencies. Nonlinear power dependence of the photoconductivity indicates that photoinduced effects play an important role in LCMO. Direct evidence for change of optical parameters under irradiation is seen by SHG transients in LCMO film [Figs. 4(a,b)]. The inset of Fig. 4(a) reveals unusual dynamics of SHG, measured in $sp(A_{\text{sp}})$ - and $pp(A_{\text{pp}})$ -polarization combinations, namely, A_{sp} signal vanishes within 20–30 s after the shutter was opened. Similar behavior was observed for ps and ss combinations; however, their very low intensity complicates any quantitative analysis. A_{pp} signal also decreases somewhat during 10 s after the shutter is opened [see Fig. 4(b)], but afterwards it increases and saturates within the next 30 s. Optical transmission T (absorption, α) decreases (increases) and saturates after about $t_s \sim 20\text{ s}$ of the irradiation [Fig. 4(c)]. Maximal relative change of the absorption $\Delta\alpha/\alpha = [T(0) - T(t_s)] / T(0)$ reaches 10–15% for ferromagnetic state.

We observed very large photoinduced changes in electrical resistivity, optical absorption, and SHG in LCMO films under laser irradiation. Their temperature behavior, shown in

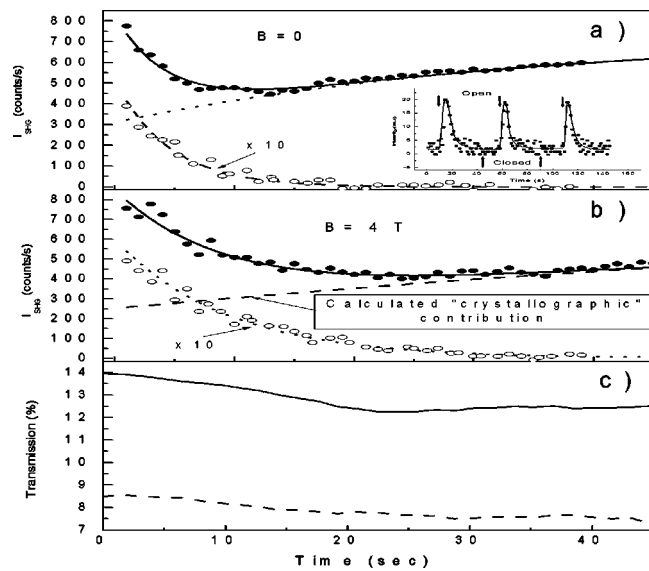


FIG. 4. Time dependences of the SHG in the p -in, p -out (solid symbols) and s -in, p -out (open symbols, multiplied by 10) polarization combinations at $B=0$ (a) and $B=4$ T (b) for a LCMO film at $T=90$ K. Lines in (b) and (c) are fits to data with superposition of exponential decay and growth. (c) Optical transmission (p -in, p -out) for $\lambda_{\omega}=760$ nm (c) at $B=0$ and $T=90$ K. In (c) solid and dash curves relate to the values of average power 0.5 and 0.25 W, respectively.

Fig. 5, looks qualitatively similar to that of the film magnetization $M(T)$, thus evidencing a tight coupling of the photo-induced effects with magnetic ordering. Moreover, a suppression of the A_{sp} signal under irradiation [analogously to ss signal, which represents pure magnetic contribution in SHG (Refs. 17 and 18)] indicates that photoexcitation is accompanied with demagnetization of LCMO. The photoexcited state is characterized by high resistivity for sample A and even insulating behavior for sample B. Extremely large photoconductivity in sample B is due to small thickness $d=30$ nm and to large absorption coefficient $\alpha(\lambda_{\omega}$

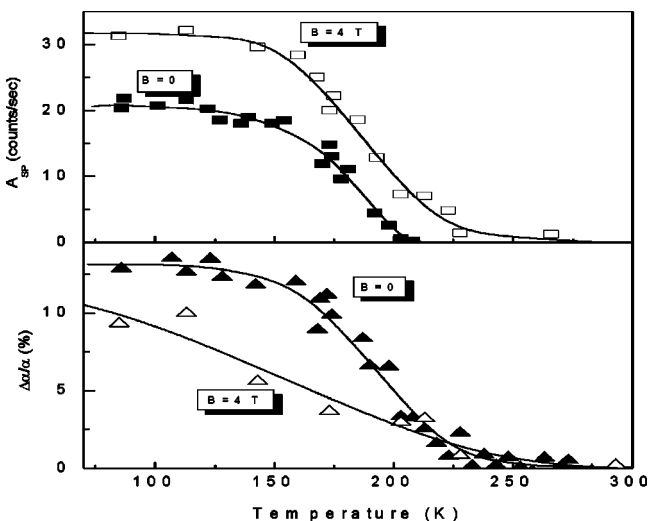


FIG. 5. Temperature dependences of the SHG (A_{sp}) and relative change of optical absorption for $B=0$ and $B=4$ T for a LCMO film.

$=760$ nm) $\sim 10^5$ cm $^{-1}$ (Ref. 19), which provide homogeneous photogeneration of extra carriers, $\Delta p \sim \beta \alpha J \tau$.²⁰ Here, β is a quantum efficiency, J the number of photons/cm 2 s, and τ the stationary lifetime of excess carriers. In the case of sample A ($d=120$ nm) generation occurs mostly in a very thin layer with $d \ll 1/\alpha$, while the rest of the film remains metallic ($T < T_C$) and shunts the surface layer. Estimated number of excess carriers Δp generated in LCMO ($T=90$ K) by means of our laser system is very large $\Delta p = (10^5)(0.8 \times 10^{14})(22) \approx 10^{20}$ cm $^{-3}$, but it is still much smaller than equilibrium carrier concentration $p = 0.33/(\text{unit cell})^3 \sim 5.6 \times 10^{21}$ cm $^{-3}$ due to Ca doping. Therefore it seems unlikely that the metal-insulator transition and demagnetization of LCMO under irradiation occurs in the same way as by increasing Ca doping from $x=0.33$ to $x=0.5$. We believe that photoexcited carriers can trigger a cooperative Jahn-Teller transformation (orbital ordering) within small clusters in accordance with the EPS picture.¹⁰ Under irradiation the size and/or number of (COI AFM) clusters increases on the expense of (metallic FM) clusters, yielding to enhanced electronic (optical) inhomogeneity of the film. Experimental support for such scenario is given by SHG transients [Fig. 4(b)], namely, magnetic contribution A_{sp} decreases down to zero within 20 s under illumination in consistence with “melting” of the (metallic FM) clusters. In contrast the “crystallographic” A_{pp} component,^{17,18} increases from a small value in dark ($t=0$) and saturates within 30 s of illumination. This behavior is in accordance with the increase of the weight of (COI AFM) clusters under irradiation. Magnetic field ($B=4$ T), favoring ferromagnetic DE interaction, inhibits the relaxation of the magnetic A_{sp} component under illumination and decreases crystallographic A_{pp} contribution [Fig. 4(b)].

Deutsche Forschungsgemeinschaft via SFB, project A2 Göttingen, and the Japanese Society for the Promotion of Science are acknowledged.

- ¹ P. Schiffer *et al.*, Phys. Rev. Lett. **75**, 3336 (1995).
- ² H. Y. Hwang *et al.*, Phys. Rev. Lett. **75**, 914 (1995).
- ³ W. Archibald *et al.*, Phys. Rev. B **53**, 14 445 (1996).
- ⁴ C. Zener, Phys. Rev. **81**, 440 (1951).
- ⁵ A. P. Ramirez *et al.*, Phys. Rev. Lett. **76**, 3188 (1996).
- ⁶ A. Moreo, S. Yunoki, and E. Dagotto, Science **283**, 2034 (1999).
- ⁷ R. von Helmolt *et al.*, Phys. Rev. Lett. **71**, 2331 (1993).
- ⁸ J. Burgy *et al.*, Phys. Rev. Lett. **87**, 277202 (2001).
- ⁹ Y. G. Zhao *et al.*, Phys. Rev. Lett. **81**, 1310 (1998).
- ¹⁰ X. J. Liu *et al.*, Phys. Rev. B **63**, 115105 (2001).
- ¹¹ K. Matsuda *et al.*, Phys. Rev. B **58**, R4203 (1998).
- ¹² K. Miyano *et al.*, Phys. Rev. Lett. **78**, 4257 (1997).
- ¹³ Y. Okimoto *et al.*, Appl. Phys. Lett. **80**, 1031 (2002).
- ¹⁴ V. Moshnyaga *et al.*, Appl. Phys. Lett. **74**, 2842 (1999).
- ¹⁵ V. Moshnyaga, B. Damaschke, O. Shapoval, A. Belenchuk, J. Faupel, O. I. Lebedev, J. Verbeeck, G. van Tendeloo, M. Mücksch, V. Tsurkan, R. Tidecks, and K. Samwer, Nat. Mater. **2**, 247 (2003).
- ¹⁶ E. D. Mishina, A. I. Morosov, Q.-K. Yu, S. Nakabayashi, and Th. Rasing, Appl. Phys. B: Lasers Opt. **74**, 765 (2002).
- ¹⁷ T. V. Murzina, T. V. Misuryaev, A. A. Nikulin, O. A. Aktsipetrov, and J. Güdde, J. Magn. Magn. Mater. **258–259**, 99 (2003).
- ¹⁸ M. Fiebig, D. Fröhlich, Th. Lottermoser, V. V. Pavlov, R. V. Pisarev, and H.-J. Weber, Phys. Rev. Lett. **87**, 137202 (2001).
- ¹⁹ X. J. Liu, Y. Moritomo, A. Nakamura, H. Tanaka, and T. Kawai, Phys. Rev. B **64**, 100401 (2001).
- ²⁰ E. Arene and J. Baixeras, Phys. Rev. B **30**, 2016 (1984).